

# Environmental and Synthesis-Dependent Luminescence Properties of Individual Single-Walled Carbon Nanotubes

Juan G. Duque,<sup>†,\*</sup> Matteo Pasquali,<sup>‡</sup> Laurent Cognet,<sup>†,\*</sup> and Brahim Lounis<sup>†</sup>

<sup>†</sup>Centre de Physique Moléculaire Optique et Hertzienne, Université de Bordeaux and CNRS, 351 cours de la libération, Talence F-33405, France, and <sup>‡</sup>Department of Chemical and Biomolecular Engineering, Rice University, 6100 Main Street, Houston, Texas 77005

Single-walled carbon nanotubes (SWNTs) offer great potential for photonics and sensing applications. On a fundamental point of view, SWNTs constitute model systems for the study of the spatiotemporal dynamics of excited states in one-dimensional systems. Semiconducting species display luminescence resonances in the near-infrared.<sup>1</sup> Experimental and theoretical studies have shown that SWNT optical properties are excitonic in nature and involve dark and bright states in the band-edge excitonic manifold.<sup>2–7</sup> However, understanding how these excitonic states shape the optical properties of SWNTs is difficult. The luminescence properties of the nanotubes are often affected by various extrinsic factors originating from synthesis, processing methods, and environmental conditions<sup>8–12</sup> that make comparison between different published studies arduous. For example, fluorescence quantum yields measured from ensembles or single nanotubes range between 10<sup>−4</sup> and 20% in literature.<sup>1,13–20</sup> Moreover, measured luminescence lifetime of nanotubes ranges from 5 to 200 ps, with excitonic dynamics that exhibit single or multiple exponential decays depending on the report.<sup>13,14,19,21–23</sup> Recently, a clear correlation between emission intensities and spectral line-widths of individual nanotubes was observed using different suspension agents.<sup>12</sup> In another study, luminescence decays of individual nanotubes lying on a surface were correlated to their spectral line-widths.<sup>11</sup> However, a comparison of the optical properties of SWNTs regarding synthesis methods, suspension agents, and local environment is still lacking. Furthermore, the origin of the nonradiative processes dominating the exciton relaxation pathways and therefore limiting the nanotube luminescence yield

**ABSTRACT** Luminescence properties of individual (6,5) single-walled carbon nanotubes (SWNTs) were studied using continuous wave and time-resolved spectroscopy. Nanotubes synthesized by different methods (HiPco and CoMoCat) and dispersed in two different ionic surfactants were examined either in aqueous environments or deposited on surfaces. SWNT preparations leading to the highest luminescence intensities and narrowest spectral widths exhibit the longest luminescence decay times. This highlights the role of the nanotube environment and synthesis methods in the nonradiative relaxation processes of the excitonic recombination. Samples of HiPco nanotubes dispersed in sodium deoxycholate contained the brightest nanotubes in aqueous environments.

**KEYWORDS:** single-walled carbon nanotubes · luminescence · spectroscopy · single molecule detection · luminescence decays · defects

is still unclear. Here we correlate photoluminescence (PL) spectra and decays obtained from individual nanotubes to identify different extrinsic factors which deeply influence their luminescence properties.

We compared the PL intensity and spectral line width of individual (6,5) SWNTs synthesized using HiPco or CoMoCat methods and dispersed in aqueous suspensions of the anionic surfactants sodium dodecylbenzenesulfonate (SDBS) or sodium deoxycholate (DOC). Two distinct HiPco batches (named herein HiPco-A and HiPco-B) were studied. All samples were prepared using brief tip ultrasonication (~10 s) in 1 weight percent (wt %) of DOC or SDBS. This procedure produces suspensions of bright and relatively long tubes.<sup>8,17</sup> The SWNTs were immobilized in aqueous agarose gels (5 wt %). The preparation was sandwiched between a glass coverslip and a glass slide and mounted on an inverted microscope. In all measurements, we selected (6,5) SWNTs (peak emission ~980 nm) by exciting them at their second order excitonic resonance<sup>24</sup> ( $E_{22} = 567$  nm). We used wide-field illumination by focusing the beam of a dye laser into the back aperture of a high NA objective, with excitation intensities below 1 kW/cm<sup>2</sup> of circularly polarized light. The

\*Address correspondence to [lcognet@u-bordeaux1.fr](mailto:lcognet@u-bordeaux1.fr).

Received for review April 21, 2009 and accepted July 02, 2009.

Published online July 13, 2009.  
10.1021/nn9003956 CCC: \$40.75

© 2009 American Chemical Society

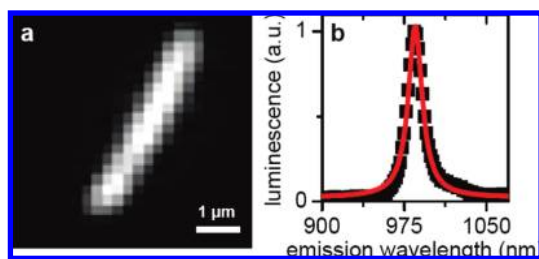


Figure 1. Wide-field luminescence image (a) and emission spectrum (b) of a (6,5) SWNT dispersed in DOC excited at its second order excitonic resonance (567 nm).

fluorescence was collected with the same objective and imaged on a low noise Si-CCD camera (Micromax, Roper Scientific) to produce wide-field images of the nanotubes. SWNTs concentration was adjusted such that bright individual nanotubes could be optically resolved (Figure 1a). The fluorescence of these bright tubes was sent to a cryogenically cooled 1D InGaAs detector (OMA V, Roper Scientific) placed at the output of a spectrometer; only individual (6,5) nanotubes were studied (Figure 1b). To avoid nanotube end and length-dependent effects which could affect comparisons between the PL properties of ensembles of SWNTs with different length distributions, we exclusively studied diffraction limited segments situated in the center of individual long nanotubes.

First, we observe that the positions of the emission lines depend on the surfactant and not on the nanotube synthesis method<sup>21</sup> ( $985 \pm 2$ ,  $986 \pm 2$ , and  $987 \pm 2$  nm for the HiPco-A, HiPco-B, and CoMoCat samples in DOC, respectively, and  $978 \pm 2$ ,  $977 \pm 2$ , and  $979 \pm 2$  nm for the same samples in SDBS). This  $\sim 8$  nm shift of the peaks in DOC is consistent with previous ensemble measurements.<sup>25</sup> Figure 2 shows the histograms of the signal peak intensities corresponding to the brightest pixels measured in the nanotube images (a–c) and of the emission lines full-width at half maxima (fwhm) (d–f) originating from individual (6,5) SWNTs dispersed in DOC. The signal peak intensities are averaged over 10 consecutive frames and normalized by the excita-

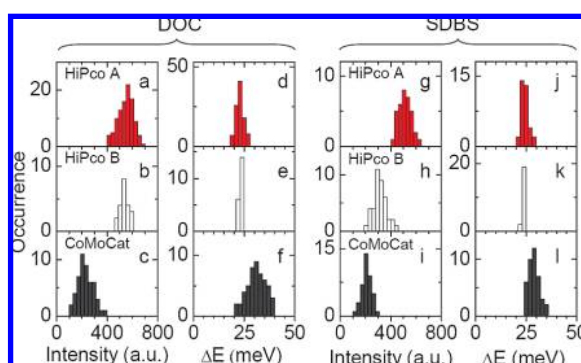


Figure 2. Histograms of the signal intensities and emission line-widths (fwhm),  $\Delta E$ , of individual (6,5) SWNTs dispersed in DOC (a–f) and in SDBS (g–l). Red corresponds to HiPco-A nanotubes, white to HiPco-B nanotubes, and gray to CoMoCat nanotubes. All measurements were performed with nanotubes immobilized in aqueous gels.

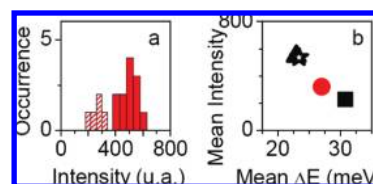
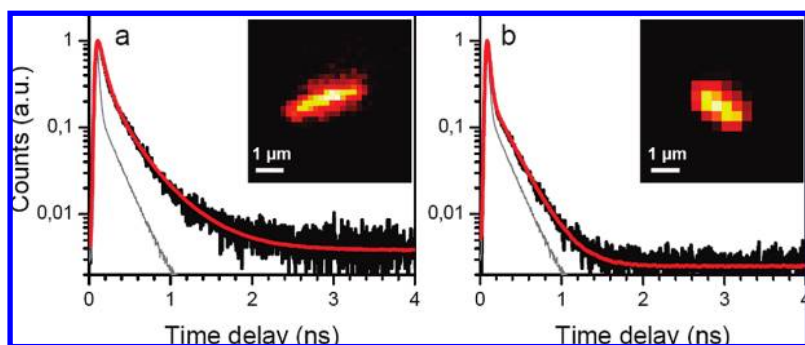


Figure 3. (a) Comparison of the signal intensities of SWNTs dispersed in DOC and studied either in aqueous gels (filled) or spincoated on a glass coverslip (hatched). (b) Mean emission intensity as a function of the mean emission line width,  $\Delta E$ , obtained from HiPco-A (triangle), HiPco-B (star), or CoMoCat (circle) nanotubes in aqueous gels and HiPco-A (square) on surfaces. All types of nanotubes were dispersed in DOC.

tion intensity. Peak intensities recorded on HiPco SWNTs were approximately twice as large as CoMoCat ones; these brighter nanotubes displayed narrower spectra.<sup>12</sup> These differences between HiPco and CoMoCat nanotubes were also observed in SDBS samples. Interestingly, in SDBS the average signal peak intensities depended on the HiPco production batches (Figure 2 g–l). The differences in luminescence line-widths and intensities observed above is likely due to different amounts of sidewall defects<sup>26</sup> introduced during the distinct synthesis and processing steps of HiPco and CoMoCat nanotubes and also to variations of the local environments of the nanotubes.<sup>21</sup> In this context, the presence of deep excitonic states discussed previously<sup>10</sup> and that occur depending on the environment, might contribute to the different line-widths observed here, as well as to the slight asymmetry of the emission lines often observed in our emission spectra (Figure 1b).

To further investigate the influence of the nanotube environments, we studied the luminescence properties of HiPco-A nanotubes suspended in DOC and spincoated onto bare or polylysine precoated<sup>27</sup> coverslips. As previously observed, and in contrast to nanotubes immobilized in agarose gels at pH above 7,<sup>28</sup> the resulting luminescence was subject to substantial blinking.<sup>29</sup> The proximity of the glass surface also resulted in lower signal peak intensities and broader emission lines than for nanotubes in aqueous environments (Figure 3a). Finally, we studied the correlation between the nanotube luminescence intensities and emission line-widths. Figure 3b reports the mean value of the luminescence intensities as a function of the mean spectral line width for the samples studied in the different conditions. Clearly, narrower emission line-widths correspond to higher emission intensities.<sup>12</sup>

Nonradiative processes, which restrain the nanotube luminescence yield, should also depend on synthesis methods, suspension agents, and local environment. To confirm this hypothesis we performed individual SWNT luminescence decay measurements on a new set of nanotubes originating from the samples studied above. The nanotubes were now excited in a confocal setup using either a continuous wave (cw) dye laser or an optical parametric oscillator (567 nm wave-



**Figure 4.** Luminescence decays and confocal luminescence images (insets) of (6,5) SWNTs excited at their second order excitonic resonance (567 nm): (a) HiPco and (b) CoMoCat nanotubes dispersed in DOC and studied in gels.

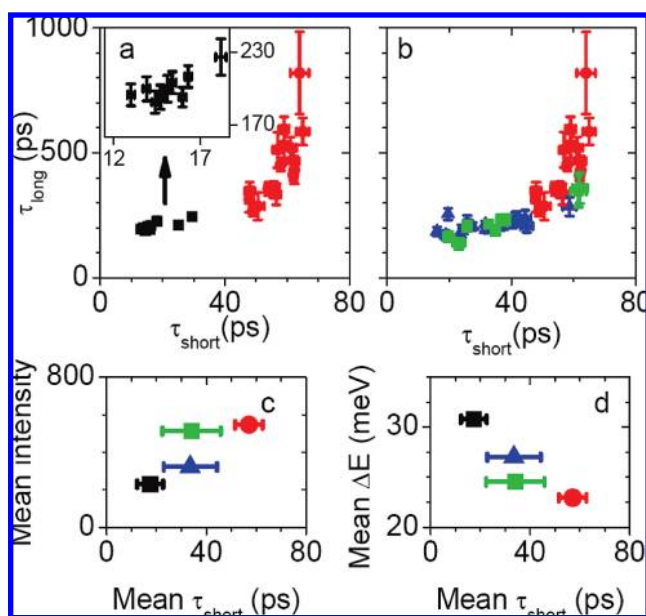
length,  $\sim 150$  fs pulses, 76 MHz repetition rate). Images were obtained in confocal mode by sending the luminescence of the individual nanotubes onto a silicon avalanche photodiode and by raster scanning the sample with a piezoscanning stage (inset of Figure 4). After identification of the (6,5) species by their emission spectrum measured under cw excitation, the luminescence decays were recorded under pulsed excitation using a conventional time-resolved single-photon counting scheme.

Figure 4 shows representative luminescence decays of (6,5) SWNT obtained in 10 min integration time with low excitation fluence ( $\sim 10^{12}$  photons/pulse/cm $^2$ ). Given the resonant absorption cross-section<sup>19</sup> of the nanotubes ( $\sim 10^{-17}$  cm $^2$  per carbon atom), less than one photon is absorbed per pulse ensuring that multiexcitonic effects are absent. Moreover, we confirmed that the PL intensity of the nanotubes stays constant during the acquisition time. All nanotubes displayed biexponential decays<sup>19</sup> with short components ( $\tau_{\text{short}}$ ) ranging between 10 and 65 ps and long ones ( $\tau_{\text{long}}$ ) from 200 up to 800 ps. Figure 5a compares the decays of nanotubes synthesized by the two different methods and dispersed in identical surfactants (DOC). CoMoCat tubes (black squares) have the fastest decay times, with narrow distributions centered on  $\sim 15$  ps for  $\tau_{\text{short}}$  and  $\sim 200$  ps for  $\tau_{\text{long}}$ . In contrast, HiPco tubes (red dots) displayed the slower decays ( $\tau_{\text{short}} = 45\text{--}65$  ps and  $\tau_{\text{long}} = 200\text{--}800$  ps). Figure 5b shows the influence of the immediate environment of HiPco-A nanotubes on the luminescence decays of DOC nanotubes in gels (red dots, Figure 5b) or spin-coated on a glass surface (green squares, Figure 5b), and SDBS nanotubes in gels (blue triangle, Figure 5b). Whereas DOC nanotubes in gels displayed the slowest decay times (for both components), DOC nanotubes lying on surfaces or SDBS nanotubes in gels displayed a narrow distribution of  $\tau_{\text{long}}$  (centered on  $\sim 200$  ps) and a broad distribution of  $\tau_{\text{short}}$  with values systematically lower than that of DOC nanotubes in gels. The presence of the gels could in principle contribute to the environmental effects influencing the luminescence properties of SDBS and DOC nanotubes. We believe that this effect should be negligible since low gel concentrations are used and no differences in the intensity and spectral

properties of nanotubes freely diffusing in water or immobilized in aqueous gels are found (data not shown).

The origin of the two decay times was previously attributed to the presence of two closely lying dark and bright excitonic states.<sup>5,6,19</sup> Weak PL yields of the bright state (limited to a few percent<sup>15–19</sup>) are due to non-radiative relaxation pathways (occurring in the tens of ps

range) which are much faster than the radiative recombination time (in the ns range). In Figures 5c,d, for each synthesis and environmental condition described above we plot the mean intensities and line-widths derived from the distributions presented in Figures 2–3 against the mean decay times deduced from Figure 5a,b. Conditions leading to the longest decay times provide the brightest and narrowest emission lines. This indicates that the synthesis methods, suspension agents and local environments impact nonradiative processes in SWNTs. They are for instance more prominent for CoMoCat nanotubes than for HiPco, probably because of the postprocessing procedure undergone by CoMoCat nanotubes.<sup>30</sup> On the other hand, the large heterogene-



**Figure 5.** (a) Long decay times as a function of short ones, deduced luminescence decays of individual (6,5) SWNTs dispersed in DOC and studied in aqueous gels: (black) CoMoCat; (red) HiPco-A. (b) Same as panel a but for HiPco-A nanotubes either dispersed in DOC and studied in aqueous gels (red circles) and on surfaces (blue triangles), or dispersed in SDBS and studied in aqueous gels (green squares). (c) Mean emission intensity (c) or emission line width,  $\Delta E$ , (d) as a function of the mean short decay time for nanotubes dispersed in DOC: HiPco-A studied in aqueous gels (red circle), on surfaces (blue triangle), or CoMoCat studied in aqueous gels (black square), as well as HiPco-A dispersed in SDBS studied in aqueous gels (green square).

ity observed for as-produced HiPco nanotubes is likely due to the presence of catalyst impurities.<sup>31</sup>

In conclusion we have established that brightly luminescent nanotubes display narrow PL spectral widths and long luminescence decay times. In this study, samples consisting of as-produced (unpurified) (6,5) HiPco nanotubes individualized in DOC and immobilized in aqueous gels provide nanotubes displaying the best PL properties, as compared to nanotubes studied on glass surfaces, suspended in SDBS or produced by the CoMoCat method. These results highlight the importance of controlling the environmental effects and synthesis methods in understanding the fundamental, intrinsic optical properties of SWNTs as well for optimizing these properties for applications in optoelectronics or biosensing.

**Acknowledgment.** We wish to thank H. K. Schmidt for helpful discussions. This research was funded by the Région Aquitaine and the Agence Nationale pour la Recherche (ANR), the NSF Center for Biological and Environmental Nanotechnology (EEC-0118007 and EEC-0647452), and the Welch Foundation (grant C-1668). J.D. thanks the Wagoner Foreign Study Scholarship and the FAME program (Bordeaux) for financial support.

## REFERENCES AND NOTES

- O'Connell, M. J.; Bachilo, S. M.; Huffman, C. B.; Moore, V. C.; Strano, M. S.; Haroz, E. H.; Rialon, K. L.; Boul, P. J.; Noon, W. H.; Kittrell, C., *et al.* Band Gap Fluorescence from Individual Single-Walled Carbon Nanotubes. *Science* **2002**, *297*, 593–6.
- Wang, F.; Dukovic, G.; Brus, L. E.; Heinz, T. F. The Optical Resonances in Carbon Nanotubes Arise from Excitons. *Science* **2005**, *308*, 838–41.
- Perebeinos, V.; Tersoff, J.; Avouris, P. Scaling of Excitons in Carbon Nanotubes. *Phys. Rev. Lett.* **2004**, *92*, 257402.
- Spataru, C. D.; Ismail-Beigi, S.; Benedict, L. X.; Louie, S. G. Excitonic Effects and Optical Spectra of Single-Walled Carbon Nanotubes. *Phys. Rev. Lett.* **2004**, *92*, 077402.
- Mortimer, I. B.; Nicholas, R. J., Role of Bright and Dark Excitons in the Temperature-Dependent Photoluminescence of Carbon Nanotubes. *Phys. Rev. Lett.* **2007**, *98*, 027404.
- Shaver, J.; Kono, J.; Portugall, O.; Krstic, V.; Rikken, G.; Miyauchi, Y.; Maruyama, S.; Perebeinos, V. Magnetic Brightening of Carbon Nanotube Photoluminescence Through Symmetry Breaking. *Nano Lett.* **2007**, *7*, 1851–5.
- Luer, L.; Hoseinkhani, S.; Polli, D.; Crochet, J.; Hertel, T.; Lanzani, G. Size and Mobility of Excitons in (6,5) Carbon Nanotubes. *Nat. Phys.* **2009**, *5*, 54.
- Cognet, L.; Tsyboulski, D. A.; Rocha, J. D.; Doyle, C. D.; Tour, J. M.; Weisman, R. B. Stepwise Quenching of Exciton Fluorescence in Carbon Nanotubes by Single-Molecule Reactions. *Science* **2007**, *316*, 1465–8.
- Lefebvre, J.; Finnie, P. Excited Excitonic States in Single-Walled Carbon Nanotubes. *Nano Lett.* **2008**, *8*, 1890–5.
- Kiowski, O.; Arnold, K.; Lebedkin, S.; Hennrich, F.; Kappes, M. M. Direct Observation of Deep Excitonic States in the Photoluminescence Spectra of Single-Walled Carbon Nanotubes. *Phys. Rev. Lett.* **2007**, *99*, 237402.
- Gokus, T.; Hartschuh, A.; Harutyunyan, H.; Allegrini, M.; Hennrich, F.; Kappes, M.; Green, A. A.; Hersam, M. C.; Araujo, P. T.; Jorio, A. Exciton Decay Dynamics in Individual Carbon Nanotubes at Room Temperature. *Appl. Phys. Lett.* **2008**, *92*, 153116.
- Tsyboulski, D. A.; Bakota, E. L.; Witus, L. S.; Rocha, J.-D. R.; Hartgerink, J. D.; Weisman, R. B. Self-Assembling Peptide Coatings Designed for Highly Luminescent Suspension of Single-Walled Carbon Nanotubes. *J. Am. Chem. Soc.* **2008**, *130*, 17134–40.
- Wang, F.; Dukovic, G.; Brus, L. E.; Heinz, T. F. Time-resolved Fluorescence of Carbon Nanotubes and Its Implication for Radiative Lifetimes. *Phys. Rev. Lett.* **2004**, *92*, 177401.
- Jones, M.; Engtrakul, C.; Metzger, W. K.; Ellingson, R. J.; Nozik, A. J.; Heben, M. J.; Rumbles, G. Analysis of Photoluminescence from Solubilized Single-Walled Carbon Nanotubes. *Phys. Rev. B* **2005**, *71*, 115426.
- Crochet, J.; Clemens, M.; Hertel, T. Quantum Yield Heterogeneities of Aqueous Single-Wall Carbon Nanotube Suspensions. *J. Am. Chem. Soc.* **2007**, *129*, 8058.
- Carlson, L. J.; Maccagnano, S. E.; Zheng, M.; Silcox, J.; Krauss, T. D. Fluorescence Efficiency of Individual Carbon Nanotubes. *Nano Lett.* **2007**, *7*, 3698–703.
- Tsyboulski, D. A.; Rocha, J. D. R.; Bachilo, S. M.; Cognet, L.; Weisman, R. B. Structure-Dependent Fluorescence Efficiencies of Individual Single-Walled Carbon Nanotubes. *Nano Lett.* **2007**, *7*, 3080–5.
- Lefebvre, J.; Austing, D. G.; Bond, J.; Finnie, P. Photoluminescence Imaging of Suspended Single-Walled Carbon Nanotubes. *Nano Lett.* **2006**, *6*, 1603–8.
- Berciaud, S.; Cognet, L.; Lounis, B. Luminescence Decay and the Absorption Cross Section of Individual Single-Walled Carbon Nanotubes. *Phys. Rev. Lett.* **2008**, *101*, 077402.
- Ju, S.-Y.; Kopcha, W. P.; Papadimitrakopoulos, F. Brightly Fluorescent Single-Walled Carbon Nanotubes via an Oxygen-Excluding Surfactant Organization. *Science* **2009**, *323*, 1319–1323.
- Hirori, H.; Matsuda, K.; Miyauchi, Y.; Maruyama, S.; Kanemitsu, Y. Exciton Localization of Single-Walled Carbon Nanotubes Revealed by Femtosecond Excitation Correlation Spectroscopy. *Phys. Rev. Lett.* **2006**, *97*, 257401.
- Berger, S.; Voisin, C.; Cassabois, G.; Delalande, C.; Roussignol, P.; Marie, X. Temperature Dependence of Exciton Recombination in Semiconducting Single-Wall Carbon Nanotubes. *Nano Lett.* **2007**, *7*, 398–402.
- Scholes, G. D.; Tretiak, S.; McDonald, T. J.; Metzger, W. K.; Engtrakul, C.; Rumbles, G.; Heben, M. J. Low-Lying Exciton States Determine the Photophysics of Semiconducting Single Wall Carbon Nanotubes. *J. Phys. Chem. C* **2007**, *111*, 11139–49.
- Bachilo, S. M.; Strano, M. S.; Kittrell, C.; Hauge, R. H.; Smalley, R. E.; Weisman, R. B. Structure-Assigned Optical Spectra of Single-Walled Carbon Nanotubes. *Science* **2002**, *298*, 2361–6.
- Arnold, M. S.; Green, A. A.; Hulvat, J. F.; Stupp, S. I.; Hersam, M. C. Sorting Carbon Nanotubes by Electronic Structure Using Density Differentiation. *Nat. Nano* **2006**, *1*, 60.
- Habenicht, B. F.; Prezhdo, O. V. Nonradiative Quenching of Fluorescence in a Semiconducting Carbon Nanotube: A Time-Domain *ab Initio* Study. *Phys. Rev. Lett.* **2008**, *100*, 197402.
- Hogele, A.; Galland, C.; Winger, M.; Imamoglu, A. Photon Antibunching in the Photoluminescence Spectra of a Single Carbon Nanotube. *Phys. Rev. Lett.* **2008**, *100*, 217401.
- Cognet, L.; Tsyboulski, D. A.; Weisman, R. B. Subdiffraction Far-Field Imaging of Luminescent Single-Walled Carbon Nanotubes. *Nano Lett.* **2008**, *8*, 749–753.
- Matsuda, K.; Kanemitsu, Y.; Irie, K.; Saiki, T.; Someya, T.; Miyauchi, Y.; Maruyama, S., Photoluminescence Intermittency in an Individual Single-Walled Carbon Nanotube at Room Temperature. *Appl. Phys. Lett.* **2005**, *86*, 123116.
- Bachilo, S. M.; Balzano, L.; Herrera, J. E.; Pompeo, F.; Resasco, D. E.; Weisman, R. B. Narrow (*n,m*)-Distribution of Single-Walled Carbon Nanotubes Grown Using a Solid Supported Catalyst. *J. Am. Chem. Soc.* **2003**, *125*, 11186–7.
- Nikolaev, P.; Bronikowski, M. J.; Bradley, R. K.; Rohmund, F.; Colbert, D. T.; Smith, K. A.; Smalley, R. E. Gas-Phase Catalytic Growth of Single-Walled Carbon Nanotubes from Carbon Monoxide. *Chem. Phys. Lett.* **1999**, *313*, 91.